Russian Chemical Reviews **71** (4) 315 – 327 (2002) © 2002 Russian Academy of Sciences and Turpion Ltd

DOI 10.1070/RC2002v071n04ABEH000710

Chemical aspects of implantation of high-energy ions into polymeric materials

D V Sviridov

Contents

I.	Introduction	315
II.	Peculiarities of the interaction of high-energy ions with polymeric target	315
III.	Chemical processes occurring during ion bombardment of polymers	316
IV.	Peculiarities of the morphology and properties of ion-implanted layer	319
V.	Prospects for practical applications of ion-implanted polymers	323
VI.	Conclusion	324

Abstract. Data on the study of the influence of accelerated ion beams on polymeric materials are generalised. The mechanisms of chemical processes occurring in a polymer matrix upon ion implantation and resulting in crucial changes in the electrical conductivity, microhardness, hydrophilicity and other characteristics of the irradiated polymer surface are discussed. Main fields of applications of ion-implanted polymeric materials are considered. The bibliography includes 188 references.

I. Introduction

Long-term ion bombardment of a polymer causes important transformations of the material, accompanied by the formation of specific modifications of amorphous hydrogenated carbon which exhibits conducting properties. Ion irradiation is also responsible for an increase in the conductivity of initially dielectric polymers (*e.g.*, polyimide and polyethylene) by 10 to 15 and even 18 orders of magnitude. Studies carried out in the last decade allowed one to gain a deeper insight into the mechanisms of ion bombardment induced processes in polymeric materials and showed that varying the main parameters of ion irradiation (energy and mass of implanted ions, implantation dose, ionic current) has a significant effect on the formation of a carbonaceous phase in the implanted layer. These studies also revealed the possibility of effective control of not only conducting and optical, but also tribological, hydrophilic and hydrophobic properties of the irradiated polymer surface.

Salient features of ion implantation into polymeric targets have been reviewed.[1–6] However, the emphasis was placed on systematisation of the data on the nature of the conducting properties of ion-implanted polymers. This review (i) concerns the character and mechanisms of chemical reactions occurring in the polymer matrix during ion irradiation to high fluences and (ii) analyses the role of these processes in the formation of the properties of ion-implanted layers formed at the surface of polymeric materials.

D V Sviridov Institute of Physicochemical Problems, Belarussian State University, ul. Leningradskaya 14, 220050 Minsk, Belarus.
Fax (37-517) 226 55 67. Tel. (37-517) 209 51 80.
E-mail: sviridov@bsu.by

Received 31 January 2002
Uspekhi Khimii **71** (4) 363 – 377 (2002); translated by A M Raevsky

II. Peculiarities of the interaction of high-energy ions with polymeric target

Specific effects of ion irradiation on polymeric samples are first of all due to very high density of energy transferred to the irradiated target. Energy loss of incident ions in polymer matrices can be as high as tens and even hundreds of electron-volts per 1 Å of track length. Energy deposition occurs within a very small volume along the ion track and takes a very short time ($\sim 10^{-13}$ s).[7] Taking into account the fact that the bond dissociation energies in polymers do not exceed 10 eV (*e.g.*, 4.3 eV for the C–H and 9.3 eV for the C=N bond), the energy deposited by the stopping projectile is high enough to break a large number of chemical bonds within the track volume even in the case of implantation of ions with medium energies (from tens to hundreds of kiloelectron-volts). This, in turn, creates prerequisites for essential transformations in the irradiated polymer during ion bombardment.

The character of chemical processes induced in the polymer matrix by ion implantation is strongly affected by two fundamentally different mechanisms of energy transfer from the incident ions to the polymer, namely, by inelastic (electronic excitations) and elastic (nuclear) collisions.[7] The former mechanism leads to excitation and ionisation of polymer molecules and (also as a result of fast subsequent neutralisation) to the formation of a large number of mobile radical species (first of all, $H^{\bullet}$ radicals) and macroradicals. Nuclear collisions are accompanied by massive rupture of chemical bonds due to displacement of atomic nuclei and by transfer of rather high energy to the polymer matrix in the form of phonons.[7] Once the deposited energy is sufficiently high, the displaced atoms can, in turn, create their own track cascades.[1,7] The contribution of each mechanism to the overall energy loss of an incident ion is characterised by its stopping power, S_n (for 'nuclear') and S_e (for 'electronic' energy loss), which represents the change in the ion energy caused by its interaction with the polymer matrix per unit path length. The S_n and S_e values depend on the energy and mass of incident ions. High-energy light ions deposit their energy mostly by electronic excitations, while heavy ions lose their energy nearly completely by nuclear collisions.[7,8] As the ion slows down, the contribution of each mechanism to the overall energy loss substantially changes (*e.g.*, a feature of the implantation of light-element ions is an increase in the relative weight of 'nuclear' energy loss at the end of the ion track [7,8]).

Thus, stopping of ions is accompanied by deposition of rather high energy within the ion tracks and is followed by the formation of radicals, secondary ions and electrons. A certain fraction of

electrons (the so-called δ-electrons) have energies high enough to escape the primary ion track.[7,9] The tracks of δ-electrons (secondary tracks) form a region called 'penumbra'[10] in which the excitation and ionisation of the polymeric material also occurs. For ions with energies of the order of 100 keV to 1 MeV per nucleon, the radius of the primary track lies between 5 and 10 Å[11] while the penumbra radius can reach 50 to 100 Å (this estimate was obtained for water which differs only slightly in stopping power from most polymers).[10,11] Compared to the ion track, the density of energy deposited in the penumbra is an order of magnitude lower[1,9–11] and the processes occurring in this region can be considered as pure radiation processes. Energy deposition occurs mainly within the track core which is thus heated to very high temperatures. Heating is due to electrons confined within the track by a strong electric field[12] perpendicular to the track axis and to direct transfer of vibrational energy to polymer by nuclear collisions.[7] The 'thermal spike' model allows estimation of temperature within a cylindrical track as a function of the radial distance (r) and time (t) elapsed after passage of an ion as follows:[13–16]

$$T(r,t) = \frac{T_0}{1 + 4\delta t/r_0^2} \exp\left[-\frac{(r/r_0)^2}{1 + 4\delta t/r_0^2}\right],$$

$$T_0 = \frac{S}{\pi \rho C_V r_0^2},$$

where T_0 is the initial temperature (at the instant the thermal spike is created), δ is the thermal diffusivity of the condensed medium in which the ion slows down, r_0 is the radius of the ion track, S is the overall stopping power for the incident ion, ρ is the density of the polymer and C_V is the heat capacity of the polymer. The T_0 values corresponding to the implantation of ions with energies ranging from 0.1 to 1 MeV into various polymers can be as high as $\sim 10^4$ K, while quenching of the track down to the temperature of a polymeric target under ion irradiation [$\sim 100-150$ °C (see Refs 17 and 18)] takes $10^{-9}-10^{-10}$ s. This formula provides only a rough estimate of the parameters of the thermal pulse produced upon passage of a high-energy ion; nevertheless, it allows one to estimate the main parameters (including the time parameters) of the thermal effects accompanying ion implantation. It should be noted that the experimental estimate of the temperature of the electron cloud created during ionisation of the atoms within the ion track can be obtained from analysis of the C (KVV) spectrum of the Auger electrons generated in the ion bombarded amorphous carbon (this is closely related to the conditions in heavily implanted polymeric materials); the theoretical estimate of the T_0 value is in reasonable agreement with the experimental results of these experiments.[19]

Build up of the dose of implanted ions leads to basic changes in the character of ion-induced processes. Initially, a pristine polymer is ion bombarded until accumulation of a certain dose D_f corresponding to complete coverage of the surface of the polymer sample with ion tracks. Futher implantation occurs into the polymer exposed to ion irradiation. In this case, the processes in the polymeric target represent a specific kind of pulse thermoradiolysis since the products of radiochemical reactions formed within and in the vicinity of the track region and those accumulated in the polymer matrix during previous irradiation are involved in the thermally induced reactions occurring in the thermal spike.

III. Chemical processes occurring during ion bombardment of polymers

Studies of the effect of ion irradiation on various polymeric materials showed that implantation to high doses leads to carbonisation of the surface of the polymer sample and to the formation of specific surface forms of amorphous hydrogenated carbon.[20–24] Carbonisation occurs efficiently if the energy loss per unit track length (or the linear energy transfer, LET) of incident ions exceeds a particular threshold value (15 to 20 eV Å^{-1} for aliphatic polymers[1]). Accumulation of carbon in the implanted layer is accompanied by evolution of a large amount of dihydrogen (usually, the major gaseous product of ion implantation), low-molecular-mass hydrocarbons (first of all, acetylene) and CO and CO_2 in the case of oxygen-containing polymers (Table 1).[1,24–28]

Table 1. Relative yields of molecular products formed during irradiation of polymer surface with 200 keV He^+ ions.[1,24]

Molecular species (fragment)	Polyethylene	Polystyrene	Polyimide
H_2	1[a]	1[b]	1
CH_4	0.02	0.01	–
C_2H_2	0.11	0.53	0.05
C_3H_5	0.01	0.004	–
C_6H_6	–	0.013	–
CO			2
CO_2			1

Note. All values were normalised to the yield of dihydrogen.
[a] The absolute yield is 4.8 hydrogen molecules per 100 eV adsorbed by the polymeric target.[1]
[b] The absolute yield is 1.15 hydrogen molecules per 100 eV adsorbed by the polymeric target.[1]

The amount of gaseous products formed in ion-induced, radiochemical pyrolytic processes exponentially decreases as the surface of a polymeric target is covered by ion tracks:[1,5]

$$Q = Q_0 \exp(-\varepsilon D),$$

where Q_0 and Q are the initial and current yields of the detected gaseous product, respectively; ε is the cross-section of the reaction accompanied by gas evolution (based on the ε value, one can estimate the reaction volume in which ion-induced thermoradiolysis occurs); and D is the implantation dose. Clearly, the ε^{-1} value allows estimation of D_f for a polymer irradiated under particular implantation regime.[1,5] For ions with energies of the order of hundreds of kiloelectron-volts, the cross-sections of ion-induced reactions accompanied by gas evolution are $\sim 10^{-14}-10^{-15}$ cm^2 (see Refs 1, 5, 29). Since the radiation processes accompanied by evolution of dihydrogen also occur within the penumbra, the cross-section of the reaction of H_2 liberation is somewhat larger than those of the reactions of formation of hydrocarbons (CO and CO_2) released immediately in the intra-track region.[30]

The fact that radiochemical processes in the penumbra allow cross-linking of polymer chains is of great importance. For instance, the yield of cross-linking for electron beam irradiated polyethylene (this regime is analogous to the action of δ-electrons) is 3 to 5 times higher than the chain scission yield.[31] In this case, radiation-induced cross-linking of the polymer occurs even at low fluences, which are two orders of magnitude lower than D_f for medium-range energy ions.[5,32] This must strongly affect the course of ion-induced pyrolytic processes. This conclusion is, in particular, supported by the fact that, in contrast to pristine polyethylene, thermal degradation of radiochemically cross-linked polyethylene leads to the formation of a solid carbonaceous phase with pronounced semiconductor properties rather than a mixture of liquid hydrocarbons.[33]

Radiolysis products are involved in the intra-track pyrolytic processes or are accumulated within the implanted layer to be consumed at later stages of ion irradiation. High-temperature pyrolysis in the track and its immediate vicinity is accompanied by scission of polymer chains. This provides the possibility of cyclisation of radiochemically generated unsaturated linear chain fragments by the intramolecular Diels–Alder mechanism (aromatic hydrocarbons are much more stable than linear unsa-

turated hydrocarbons at temperatures above 800 °C). As the track is cooled down, the newly formed aromatic fragments and analogous fragments present in the pristine polymer and released upon thermoradiolysis are linked together, thus being stabilised due to extension of the conjugation system.[3]

According to data from mass-spectrometric analysis, the exhaust gases evolved during ion implantation include hydrogen and hydrocarbons with different molecular masses.[1,24,34] Usually, the most abundant product is acetylene which is the most stable acyclic unsaturated hydrocarbon at high temperatures. Large amounts of saturated hydrocarbons (methane, ethane) are produced by ion irradiation of polypropylene and polybutylene.[34] Despite the fact that the exhaust rate of the gases evolved can be as high as hundreds of metres per second,[16] most of them have no time to leave the heating zone during the dispersal time of the thermal spike. Evidently, a fraction of these hydrocarbons can react before escaping the track region; however, the contribution of such processes to the formation of the end products of thermoradiolysis is still to be clarified.

In deeper stages of ion implantation, polynuclear compounds (in essence, they represent primary carbon-containing cluster structures) and other thermoradiolysis products (unsaturated compounds, stable macroradicals) formed in the track region are involved in the growth of carbon clusters. For both aliphatic and aromatic polymers irradiated by ions with medium energies (hundreds of kiloelectron-volts) carbonisation of their surfaces nearly goes to completion at implantation doses of 5×10^{15} to 10^{16} cm^{-2} and subsequent ion bombardment causes only slight changes in the composition of the implanted layer.[35,36] Noteworthy is that no full carbonisation of the polymer surface occurs. For instance, implantation of polyethylene with 150 keV F^+ ions ($S_e/S_n \approx 5$) leads to an increase in the concentration of carbon in the implanted layer from 33% (in the pristine polymer) to 40%.[35]

The extent of dehydrogenation of ion irradiated polymers rapidly increases with increasing energy transferred from the incident ions by nuclear collisions. In particular, saturation of carbon concentration in the implanted layer is reached at 65% for implantation of polyethylene with 150 keV As^+ ions ($S_e/S_n \approx 0.3$).[35] If the electronic stopping mechanism dominates, dehydrogenation is of low efficiency. This can be rationalised by delocalisation of excitations over sufficiently large carbon clusters. Direct cleavage of chemical bonds upon nuclear collisions is more efficient to provide deep dehydrogenation of the polymer matrix. The extent of carbonisation that can be reached in this case is first of all controlled by the trapping of hydrogen radicals by broken carbon bonds. A profound dehydrogenation (concentration of bound hydrogen less than 10%) can be achieved with electronic deposition mechanism when ions with energies of several tens of MeV are implanted in a polymer target.[21] In this case, the formation of broken bonds, due to migration of excitations, is concentrated at the edges of growing carbon clusters and carbonaceous phase produced by high-fluence implantation exhibits the Raman spectrum similar to that of ion-implanted graphite.[21]

Implantation of high-energy ions can provide prerequisites for intra-track formation of fullerenes C_{60} and C_{70}. This is supported by the results of mass-spectrometric analysis of gaseous products evolved during implantation of poly(vinylydene chloride) with ions with energies of the order of several tens of megaelectron-volts[37] and by the data of chromatographic analysis of the products extracted from the ion-implanted layer on the surface of polyimide irradiated with 5 MeV Li^+ ions.[38,39] Taking into account modern concepts of the mechanism of fullerene formation in plasma (vapour phase),[40–45] one can assume that the synthesis of bulky carbon structures involves coalescence of polycyclic radicals (*e.g.*, combining of six perdehydronaphthalene radicals to yield the C_{60} molecule[45]). This must be favoured by shrinking of the reaction volume upon track 'collapse'.[44] Fullerene formation can also occur *via* polyynes[43] (products of deep dehydrogenation of polymers or intra-track conversion of acetylene) which lose their stability as the molecular chain is lengthened. This reaction is to be exothermic, since the enthalpy of formation of polyynes (27 kcal mol^{-1} per carbon atom[46]) is much larger than that of fullerene (9.08 kcal mol^{-1}, see Ref. 47). Accumulation of alkynyl groups in the polymer matrices irradiated with high-energy ions[48] suggests the possibility of polyyne formation during ion implantation.

The composition of the polymer matrix can strongly affect the composition of the products of ion-induced thermoradiolysis. This can be best exemplified by halogenated polyolefins. Ion irradiation of perfluorinated polyolefins results in lower unsaturated perfluorocarbons (C_2F_4, C_2F_6) as major gaseous products since the energy of the C–F bond is higher than those of the C–H and C–C bonds.[24] Because of this, detectable carbonisation of ion irradiated polytetrafluoroethylene (PTFE) can be reached only at very high doses[49] while the implantation is accompanied by erosion of the polymer sample[50] (up to perforation[24]). Ion bombardment of partially halogenated aliphatic polymers causes radical-induced dehydrohalogenation[1,18,23,27] accompanied by dehydrogenation and evolution of acetylene (Table 2). Accumulation of double bonds in the polymer matrix accelerates dehydrohalogenation and the newly formed polyenes are involved in the formation of the carbonaceous phase. It is believed that efficient ion-induced carbonisation of poly(vinyl chloride)[1,18] is favoured by the fact that thermolysis of this polymer can occur at low temperatures (~200 °C, see Ref. 51).

Table 2. Relative yields of molecular products formed during irradiation of polytetrafluoroethylene[24] and Tefzel (copolymer of ethylene and tetrafluoroethylene)[23] with 200 keV Si^+ ions.

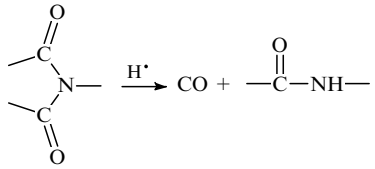
Product	PTFE	Tefzel
H_2	–	4.34
C_2H_2	–	0.87
HF	–	3.91
C_2F_4	1	1
C_2F_6	2.05[a]	0.35[a]

Note. All values were normalised to the yield of C_2F_4.
[a] Determined from the yield of the CF_3^+ fragment detected in the mass spectrum.

Ion-induced thermoradiolysis of organosilicon polymers leads to gradual accumulation of $\{SiO_4\}$ clusters at the irradiated surface due to the lack of efficient mechanisms of silicon sublimation. The loss of most of methyl groups in polymethylsiloxane as the result of bombardment with 5 keV Ar^+ leads to the formation of carbon–silicate composite, the composition of which varies from $Si_{1.3}CO_{2.0}$ at the surface to $Si_{1.5}CO_{2.5}$ in the depth, with silicon atoms in this composite being directly bound to oxygen ones.[52] Noteworthy is that implantation of a copolymer of polydimethylsilane and methylphenylsilane, $[\sim Si(CH_3)_2-SiPhCH_3\sim]_n$, with 2 MeV Ar^+ ions leads to the formation of silicon carbide as a result of cleavage of the Si–Si and C–H bonds and by elimination of methyl side groups.[53]

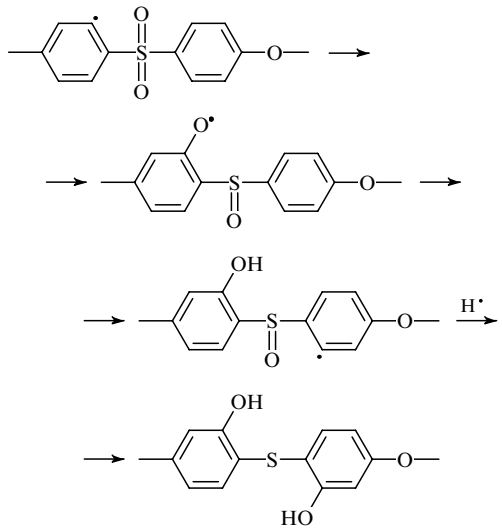
Depending on the mechanism of energy deposition by incident ions to the polymer matrix, strongly different thermoradiolysis can be induced. The distinctions are due to the fact that nuclear collisions involve direct nonselective (in essence, random) breakage of chemical bonds, whereas an electronic excitation can migrate over a rather long distance during the lifetime of the excited state (~10^{-12} s) (according to calculations for an aliphatic chain,[54] the mean path length of electronic excitation can amount to 100 monomer units) and therefore energy deposition by 'electronic' stopping implies scission of the weakest bonds. This makes possible selective initiation of chemical reactions in the polymer matrix, especially in the case of ion irradiation of heterochain polymers.

Implantation of polyimide with 90 keV N^+ ions or 150 keV Ne^+ ions ($S_e/S_n > 6.5$) leads to cleavage of bonds between aromatic rings [55] and to transformation of imido groups into amido groups without fragmentation.[56, 57]



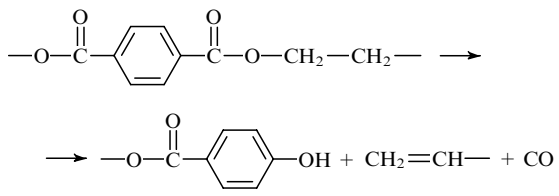
This process occurs simultaneously with dehydrogenation of polyimide and causes the loss of some carbonyl groups [58] accompanied by the evolution of CO (major gaseous product formed during ion irradiation of polyimide).[24]

A feature of the irradiation of aromatic poly(ether sulfone) under analogous conditions ($S_e \gg S_n$) is the fast transformation of sulfone groups into sulfoxide ones and then, at high fluences, into sulfide groups in the reactions involving mobile radical species $H^{\bullet}$.[6, 59]



During ion irradiation of aliphatic polysulfones the reduction of sulfone groups and their elimination in the form of sulfur dioxide occur in comparable yields.[60]

The formation of hydroxy groups in the polymer matrix was revealed in the study of low-dose ion implantation of poly(ethylene terephthalate) (PETP) under conditions where the electronic stopping prevails.[61]



This allows rapid accumulation of unsaturated groups in the ion-implanted layer on the PETP surface [these groups are accumulated in PETP faster than in, *e.g.*, poly(butylene terephthalate) [62]]. Ion-induced processes occurring during bombardment of PETP by high-energy ions (with energies of the order of several tens of megaelectron-volts and, correspondingly, with large S_e values) proceed by the same mechanism.[63] Implantation of this material with ions with energies of the order of several hundreds of megaelectron-volts leads to profound dehydrogenation of the irradiated polymer, accompanied by accumulation of alkynyl groups in the ion-implanted layer.[48] Peculiar to polystyrene and polyimide implanted in this regime is the formation of groups containing triple bonds [*e.g.*, isocyanate ($-N=C=O$) and cyanate ($-O-C\equiv N$) end groups for polyimide].[48]

Thus, if energy transfer to the polymeric target is mainly by electronic excitations, the bridging bonds are broken and functional groups undergo transformations (as a rule, towards the reduction of heteroatoms), whereas aromatic fragments remain intact and can be involved in the formation of polycyclic fused structures. Heterocycles with asymmetrical delocalised π-electron systems are much less stable. For instance, experiments on electron beam irradiation of poly(2-vinylpyridine) (in this case, energy is deposited in the polymeric target solely by electronic excitations) showed that the pyridine ring rapidly breaks down with the formation of amino groups [64] in contrast to the aromatic rings in polyimide that are stable under these conditions.[6, 64]

A consequence of the increased contribution of a collision term to the overall energy loss of the stopping ions is the change in the character of processes occurring in the polymeric target. In particular, destruction of highly stable aromatic rings is made possible. For instance, irradiation of aromatic poly(ether sulfone) with 50 keV As^+ ions ($S_n/S_e = 5.6$) causes not only the transformation of sulfone groups, but also the release of acetylene and the formation of 1,4-substituted butadiene.[65] Similarly, implantation of polyimide with ions that lose their energy mostly by nuclear collisions is accompanied by breakage of aromatic rings and formation of acetylene [24] and by nonselective degradation of imido groups resulting in the formation of various products (Fig. 1).[6, 66–68] Similar products were also detected during *in vacuo* thermal decomposition of polyimide.[67] However, their concentrations are substantially different from those in the ion-implanted layer (see Fig. 1) because these products are formed in two different ways, *viz.*, in the course of several concurrent radical processes (ion implantation) and in consecutive chemical transformations of the polymer matrix (thermal decomposition).

The overall picture of the processes occurring during ion-induced thermoradiolysis of heteroatom-containing polymers can be described as follows. Until build up of a certain implantation dose corresponding to D_f (a single track regime) the polymer matrix undergoes dehydrogenation and some other unambiguously identifiable chemical transformations. The pathways of

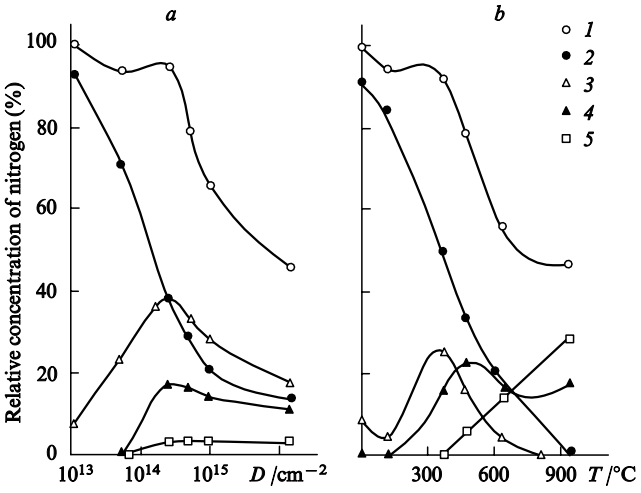
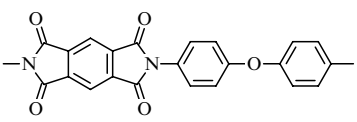


Figure 1. Changes in relative concentration of nitrogen-containing groups in polyimide  during implantation with 5 keV Ar^+ ions (*a*) and thermal decomposition (*b*) (according to XPS data).[6, 67]
Total nitrogen content (*1*), imide groups (*2*), $-C=N-$ groups (*3*), pyridine groups (*4*) and tertiary amines (*5*).

these processes are first of all determined by the ratio of energy transfer from the implanted ions by electronic excitations and by nuclear collisions. Within this implantation dose, the overall concentration of heteroatoms in the ion-implanted layer (nitrogen atoms in irradiated polyimide [6, 67] or sulfur atoms in irradiated polysulfone [6, 59]) can remain virtually constant (Figs. 1 and 2) while the energy of the implanted ions is expended for structural rearrangement of the polymer.[6] Aromatic fragments released in this stage are fused to form 'pre-carbon' structures. These processes can occur involving the heteroatoms incorporated into the pyridine, pyran and thiopyran rings. Because of this, a large fraction of heteroatoms (first of all, sulfur and nitrogen) is retained in the implanted layer in chemically bound form even at high implantation doses.[6]

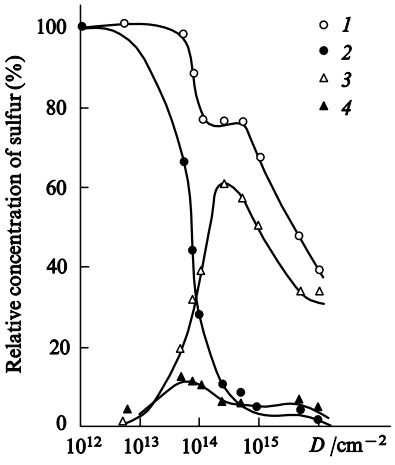


Figure 2. Changes in relative concentration of sulfur-containing groups in poly(ether sulfone) during implantation with 150 keV Ar^+ ions.[6] Total sulfur content (*1*); sulfone (*2*), sulfide (*3*) and sulfoxide (*4*) groups.

IV. Peculiarities of the morphology and properties of ion-implanted layer

Electron microscopy studies of ion-implanted polymers revealed the formation of carbon aggregates of a size up to several tens of nanometres in polymeric targets implanted with high doses.[23] Using the small-angle neutron scattering technique, it was established that these aggregates are comprised of small carbon clusters.[69] In particular, it was found that high-dose irradiation of PETP films with 50 MeV B^+ ions leads to the formation of nanoclusters of size 6 to 7 nm separated by $\sim$13 nm and united into spherulites of diameter up to 50 nm in the implanted layer.[69] This is consistent with the results obtained by optical spectroscopy, according to which the build up of implantation dose is accompanied by a shift in the edge of the optical absorption band of the irradiated polymer towards the long-wavelength region due to extension of the conjugated system in the growing carbon clusters. The magnitude of the shift indicates that the size of the clusters formed during implantation with medium energy ions is at most several nanometres.[70–72] Using an approach developed for amorphous carbon,[73] the mean size of a carbon cluster grown in the implanted layer can be estimated as follows:

$$E_g = 2|\beta|N^{-0.5},$$

where E_g is the optical gap, β is the resonance integral (according to EHT calculations, $\beta = 2.9$ eV) and N is the number of rings in the compact two-dimensional carbon cluster (fragment of graphite sheet). As the implantation dose D increases, the E_g value exponentially decreases [71, 72]

$$E_g = E_{g0} + A\exp(-\eta D),$$

where E_{g0} is the energy gap corresponding to the largest clusters that can grow under the given implantation regime, η is the cross-section of the growth reaction of carbon clusters and A is a constant. The growth rate of the carbon nanophase and the η value depend first of all on the nature of the polymer,[71] while the E_{g0} value is mainly determined by the mass and energy of ions implanted.[3, 72] Implantation of light ions with energies ranging from 100 to 300 keV into polyolefins and polystyrene saturates the E_g values at 0.6 eV,[70–72] which corresponds to clusters with a mean size of 2.7 nm ($\sim$75 rings). Peculiar to the irradiation of polyamide-6 under analogous conditions is the formation of smaller clusters ($N \sim 60$, $E_g = 0.76$ eV, see Ref. 72). The fact that there exists a limiting size of carbon clusters for a given implantation regime can be rationalised [3, 72] by delocalisation of the energy of incident ions over the carbon network and by expenditure of this energy for cleavage and formation of carbon bonds accompanied by trapping of the $H^{\bullet}$ radicals. Not counting subtle details, this produces no significant variations in the medium-range order of the implanted layer. In this case, an increase in the implantation dose causes gradual growth of small carbon clusters up to the limiting size.[70] For polyamide-6, the formation of smaller carbon clusters is a result of the incorporation of a heterocyclic nitrogen atom into the growing cluster (due to, *e.g.*, the formation of pyridine rings).[72] The outermost heteroatoms cannot play the role of nucleation sites of the carbon clusters and their presence in the clusters reduces the size of extended regions of the π-electron conjugation system and, as a consequence, the effective size of carbon clusters determined from electronic spectra.[3, 72]

An increase in the size and concentration of carbon clusters in the ion-implanted layer with the implantation dose is accompanied by an increase in the concentration of paramagnetic centres (radicals stabilised by delocalisation of their π-electrons over the π-electron system of the carbon nanophase).[25, 65, 74, 75] There is a correlation between the increase in the ESR signal during implantation and completion of dehydrogenation of the polymer matrix.[17, 29] At high implantation doses where the possibilities of further carbonisation are exhausted the prerequisites are created for compensation of the terminated carbon bonds by their recombination that results in the decrease of spin concentration.[17, 29, 65, 74, 76, 77] This effect can be readily traced for polyimide,[29] polyacrylonitrile [74] and other polymers containing a large number of groups that can be efficiently fused during thermoradiolysis. Aliphatic polymers are characterised by a much lower yield of carbon clusters compared to polymers with conjugated bonds. In this case, the spin concentration plotted as a function of implantation dose exhibits no extremum (Fig. 3) even at high fluences (10^{17} cm^{-2}).[75, 78] As the dose increases, the ESR line becomes narrower due to extension of the π-electron conjugated system in the ion-implanted layer.[29, 74, 78] Studies of temperature dependence of the ESR linewidth and of the effect of oxygen pressure on the ESR spectrum revealed the formation of quasi-two-dimensional degenerate electron gas in the carbonaceous layer on the surface of heavily implanted polymers ($D > 2 \times 10^{16}$ cm^{-2} for polyethylene and polyimide irradiated with 100 keV B^+ ions).[75, 78, 79]

A salient feature of the morphology of the ion-implanted layer is the presence of nanopores that are formed along the trajectories of projectiles. Pore mouths can be clearly seen in, *e.g.*, atomic force microscopy images of the PETP surface irradiated with low doses of heavy high-energy ions.[80] Implantation of low-energy (100–200 keV) ions is also accompanied by the formation of a developed pore system. This is indicated by the possibility of spontaneous incorporation of molecular iodine from the vapour phase [81, 82] and Pb^{2+}, Fe^{3+}, K^+ and Cl^- ions (see Refs 83–85) and some bulky molecules (a carborane complex of cobalt,[86] amino acids [87]) from aqueous solutions into the implanted layer and by the possibility of extension of the oxidation of radical

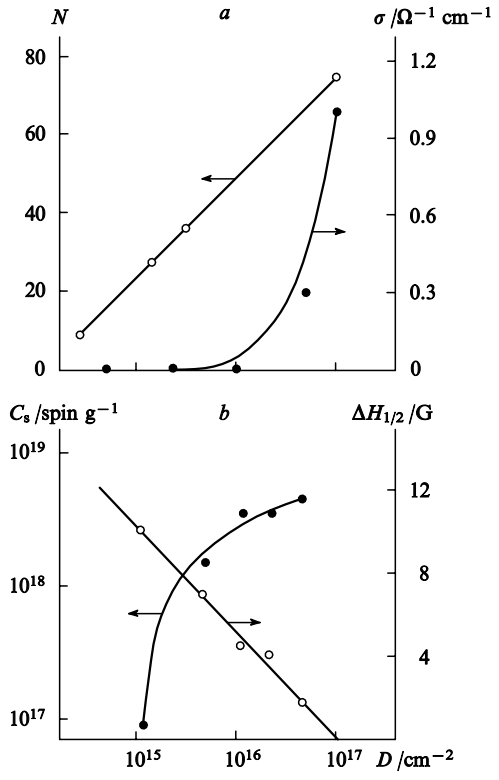


Figure 3. Dependences of the average number of carbon rings (N) in carbon cluster and of the dc conductivity (σ) (*a*), concentration of unpaired spins (C_s) and ESR linewidth (*b*) on the implantation dose for polyethylene irradiated with 100 keV B^+ ions.[75]

centres across the whole width of the implanted layer.[35, 88–90] Sometimes, changes in the polymer density along the track of the implanted ion are insufficient to ensure the pore formation. In this case, slow oxygen diffusion *via* ion-induced defects occurs along the so-called latent tracks (the regions in which locally reduced density appeared in the polymer matrix during passage of an ion). For ion irradiated polypropylene, the oxidation front propagates in the implanted layer with a velocity which does not exceed 4×10^{-5} nm s^{-1} and complete oxidation takes several weeks,[35] whereas the oxidation of polyethylene irradiated under the same regime is completed virtually immediately after the vacuum – open air transition.[35] According to IR spectroscopy data, oxygen fixation in the ion-implanted layer is accompanied by the formation of carbonyl[88, 91] and hydroxy groups.[92]

Trapped oxygen is accumulated in the domains with high density of the broken carbon bonds formed during implantation; therefore, the character of oxygen distribution in the irradiated polymer contains information on the structure of the implanted layer.[3, 35, 89, 93] Rutherford backscattering spectroscopy studies showed that the concentration of trapped oxygen in the irradiated polyethylene monotonically increases during ion irradiation[90] and reaches a maximum value at fluences of $(1-5) \times 10^{14}$ cm^{-2} for heavy ions[35, 93] and at 5×10^{15} cm^{-2} for light ions.[88] The total amount of oxygen assimilated within the implanted layer can be rather large (the concentration of oxygen in polyethylene irradiated with 150 keV F^+ ions at a fluence of 5×10^{15} cm^{-2} is 0.24 per carbon atom[88]). Using the depth profiles of oxygen trapped in the implanted layer, it was found that the role played by the 'electronic' and 'nuclear' stopping mechanisms in the generation of dangling carbon bonds is dependent on the implantation dose.[88, 93] If a pristine or slightly dehydrogenated polymer is ion irradiated, the formation of free valences in the growing carbonaceous phase is first of all a result of 'electronic' energy loss. If a partially carbonised polymer is implanted, the carbon bonds are mainly broken by nuclear collisions, whereas the energy transferred to the irradiated polymeric target by electronic excitations dissipates in carbon structures or is expended for their rearrangement. Therefore, even for irradiation with heavy ions characterised by large S_n/S_e ratios the oxygen depth profile reconstructed from the Rutherford backscattering spectra corresponds to the 'electronic' loss distribution at low fluences ($\sim 10^{14}$ cm^{-2}) and to the 'nuclear' loss distribution at higher fluences.[3, 88, 93]

At high fluences, a well-developed carbonaceous phase can form by linking individual carbon clusters. In this case, the concentration of oxygen scavengers substantially reduces and the concentration of oxygen in the implanted layer and the yield of carbonyl groups per implanted ion rapidly decrease as fluence increases.[93] The minimum concentration of trapped oxygen in the implanted layer corresponds to maximum enrichment of this layer with carbon as a result of ion-induced thermoradiolysis.[89] It should be noted that in polyethylene and polyamide-6 heavily implanted with medium-range energy (100 – 200 keV) light (*e.g.*, B^+, see Refs 94 and 95) and heavy (*e.g.*, Sb^+ and As^+, see Refs 3, 89, 93) ions the spatial region of maximum carbonisation is beneath the polymer surface.[75, 95, 96] This can be illustrated by the depth profile of the relative concentration of carbon in the near-surface layer and by the presence of an additional maximum of the concentration of trapped oxygen on the surface of irradiated samples (in this case, the oxygen depth profile exhibits two peaks, see Fig. 4). The 'buried' carbonaceous layer is separated from the surface by a layer of non-carbonised, radiation damaged polymer.[75, 94, 96] This effect can be rationalised by higher heat release at the track ends of implanted ions and by lateral spread of the thermoradiolysis zone within the collision cascade region.[3]

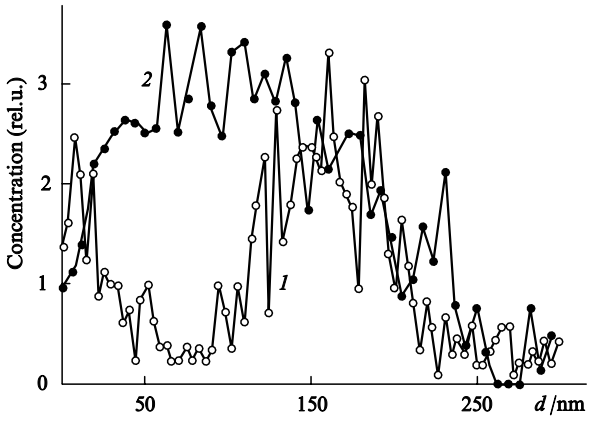


Figure 4. Depth profiles for trapped oxygen (*1*) and for an increase in the carbon concentration (*2*) in polyethylene irradiated with 150 keV As^+ ions at a fluence of 5×10^{16} cm^{-2} (according to Ref. 89).

Rutherford backscattering studies of the implant distribution (for implantation with heavy ions) and neutron depth profiles (for implantation with light ions) showed that sometimes high penetrability of the implanted layer allows the implant to diffuse out of the irradiated polymer. The pore system produced by the tracks of implanted ions provides conditions for specific gas transport reactions. In these situations the implant is either not detected[97, 98] or the experimental depth profile differs from the corresponding calculated depth profile to such a high extent[99, 100] that this can be explained by neither changes in the polymer density due to carbonisation and ion-induced erosion of the surface of the sample nor by backscattering of ions at high fluences. These effects are observed if the implant is incapable of bonding to the polymer matrix or if the interaction between the implant and matrix results in volatile products (here, heating of the polymeric target to moderate temperatures is sufficient for complete sublimation of the implant). This is characteristic of, *e.g.*, implanta-

tion of noble gas ions [97,98] and F^+ ions in polyolefins.[88] In the latter case, volatile fluorocarbons are formed. Volatile compounds are also formed during implantation of PTFE with Sb^+ ions, which is accompanied by sublimation of antimony fluorides.[49] However, if the flux of implanted ions is rather low, the noble gas ions are retained in the polymeric target (*e.g.*, Xe^+ ions in poly(ether sulfone),[21] Kr^+ ions in polyimide [101]), but they diffuse out of the ion-implanted layer with time.[102]

In the case of implantation of polymeric targets cooled down to 90 K, the depth profile of noble gas ions (in particular, xenon [103]) matches the corresponding calculated depth profile to an accuracy of 10%.

Diffusion of low-molecular-mass compounds formed in the interaction of thermalised implanted ions with the polymer matrix (including the interaction on storage) can have a significant effect on the spatial distribution of the implant. For instance, phosphorus implanted into a molecular film based on a dianthrylidene derivative of γ-substituted pyrone diffuses towards the surface of the irradiated sample (probably, in the form of phosphines). The interaction with dioxygen causes phosphorus fixation in the form of corresponding oxides.[104] As a result, the phosphorus depth profile in the implanted layer appears to be bimodal. The first maximum corresponds to medium projected range of the implanted ions while the second maximum is at the surface of the sample.[104] High mobility is also characteristic of implanted lithium (the form in which lithium is transferred is unknown). A fraction of lithium ions diffuses towards the surface of irradiated polymers.[105,106] Substantial redistribution of boron implanted into various polymers is illustrated by Fig. 5. According to XPS data, the boron escaped from the polymer bulk is oxidised.[108] The formation of volatile alkylboron compounds during implantation of boron ions has been suggested;[3] this is indicated by the fact that, according to cryochemical atomic-beam experiments,[109] elemental boron readily reacts with hydrocarbons. The interaction with dioxygen and atmospheric moisture results in volatile oxidised alkylboron compounds and alkylboric acids. This is responsible for the possibility of thermally induced desorption of implanted boron [110] and for complete disappearance of boron from the implanted layer upon long-term storage.[97]

Obtaining mobile implant at low fluences implies that the stopping ions transfer to the polymer a rather high energy (15–20 eV $Å^{-1}$, see Ref. 105) which is sufficient for occurrence of efficient thermoradiolysis and provides a necessary decrease in the density of the material of the polymeric target within the track region of implanted ions. Under these conditions, diffusion occurs nearly completely along ion tracks.[106] On the other hand, the formation of developed carbonaceous phase in heavily irradiated polymer samples creates a barrier to diffusion of the implant towards the surface.[111]

The reduction conditions which are created in the surface layer during the bombardment of a polymeric target by metal ions favours the formation of metal nanophase.[112] This process was studied taking polymethylphenylsiloxane and epoxy resins implanted with Ag^+, Fe^+ and Co^+ ions as examples (see Refs 113–118). It was found that the morphology of the newly formed metal nanophase is to a great extent controlled by the viscosity of the polymer matrix. Ion implantation of polymers in the viscous-flow state is accompanied by the formation of spherical nanoparticles with narrow size distribution, while transition of the polymer matrix to the glassy state leads to the formation of facet metal structures in the implanted layer .[114] Spherical metal nanoparticles are also formed in polyimide implanted with 150 keV copper, zinc and silver ions in high doses [$D = (1-5) \times 10^{17}$ cm^{-2}],[119,120] whereas the implantation of polyimide with W^+ ions causes the formation of a tungsten carbide nanophase.[121]

A consequence of essential structural changes in the polymer matrix, caused by ion bombardment is a substantial change in the polarity of the polymer surface (Fig. 6). This can be due to both degradation of initial (if they exist) and formation of new polar groups. The latter can be formed either immediately during implantation (for heteroatom-containing polymers) or as a result of the oxidation of radical centres due to contact with dioxygen. For instance, transformation of an imide group into an amido group during low-dose implantation of 90 keV N^+ ions into polyimide leads to a more than twofold decrease in the polar component of the surface free energy.[56] A decrease in the surface polarity was also observed in the course of ion irradiation (Sb^+, 150 keV) of polyamide-6,[49] whereas ion irradiation of PETP (N^+, 90 keV) accompanied by transformation of ester groups into hydroxy groups leads to an insignificant (by 30%) increase in the surface polarity.[61] These rearrangements of the polymer surface occur at low irradiation doses. Polarity of heavily implanted samples first of all depends on the presence of carbonyl groups formed involving uncompensated bonds of carbon atoms at the boundaries of the carbonaceous phase. For aliphatic polymers (polyethylene, polypropylene) the formation of carbonyl groups is the main factor responsible for a substantial increase in the polarity of the polymer surface at any dose.[49,88] An increase in the surface polarity of polysiloxanes after ion implantation is due to the formation of nanodispersed SiO_2 phase inclusions in the implanted layer.[52]

The sorption properties of irradiated polymers are affected by the developed system of nanopores in the implanted layer and by ion-exchange character of the sorption sites inside the pores (the

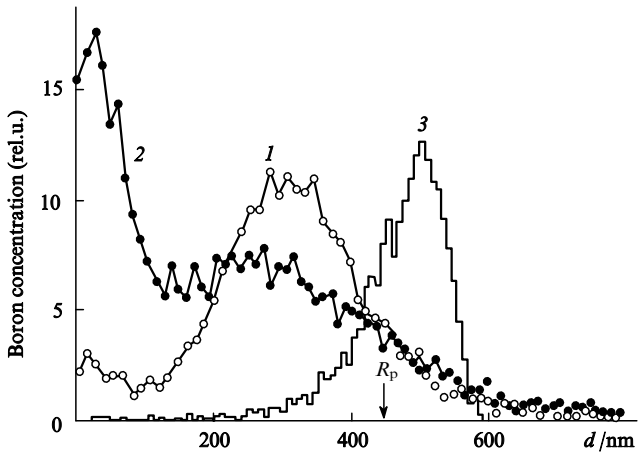


Figure 5. Boron depth profiles for polyethylene (*1*) and polyamide (*2*) irradiated with 100 keV B^+ ions ($D = 5 \times 10^{16}$ cm^{-2}, see Refs 3 and 93) and calculated depth profile for boron implanted into polyethylene (*3*) (results of Monte Carlo simulation using the TRIM code [107]). R_p is the theoretical projected range of the implanted ion.

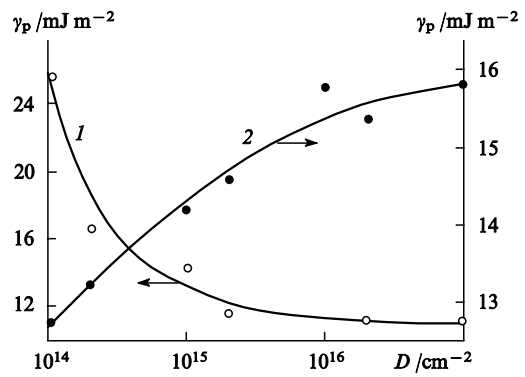


Figure 6. Polar component of the surface free energy (γ_p) of polyimide (*1*) and PETP (*2*) films irradiated with 90 keV N^+ ions plotted as a function of the implanted dose (according to Refs 56 and 61).

adsorption capacity of irradiated polyethylene and polypropylene with respect to cations is 2 to 5 times higher than with respect to anions [84, 85]).

Carbon-containing species formed during ion implantation reinforce the polymer surface. In some instances the microhardness of the irradiated surface can be substantially increased (up to 50 to 70 times [122–126]). These effects were observed for various polymers, namely, polyimide,[28, 123, 126] polystyrene,[122, 123] polyethylene,[92, 127] PETP,[28] polycarbonate $\{[\sim OC_6H_4C(CH_3)_2-C_6H_4OCO\sim]_n\}$,[128] partially fluorinated polyethylene,[23] poly(ether ether ketone) $\{[\sim OC_6H_4OC_6H_4COC_6H_4\sim]_n\}$ [129] and some other polymers irradiated with different (mostly light and not too heavy) ions with energies ranging from 100 keV to 1 MeV. The microhardness of carbonaceous products is first of all determined by the character of interconnectivity within the carbon cluster aggregates.[20] High microhardness requires that the incident ions deposit their energy mainly by electronic excitations (this provides the formation of carbon clusters) and the energy loss by nuclear collisions be relatively small. Though nuclear collisions are responsible for the formation of random links between the clusters, a general trend is towards an increase in the microhardness with an increase in the relative weight of energy loss by electronic excitations (Fig. 7).[122, 130] However, since the displacement energy of an sp^3-hybridised carbon atom (80 eV for diamond) is much higher than that of an sp^2-hybridised carbon atom (30 eV for graphite),[5] one can expect that nuclear collisions lead to gradual accumulation of domains with predominant sp^3-hybridisation of carbon atoms and increased microhardness of the ion-implanted layer.

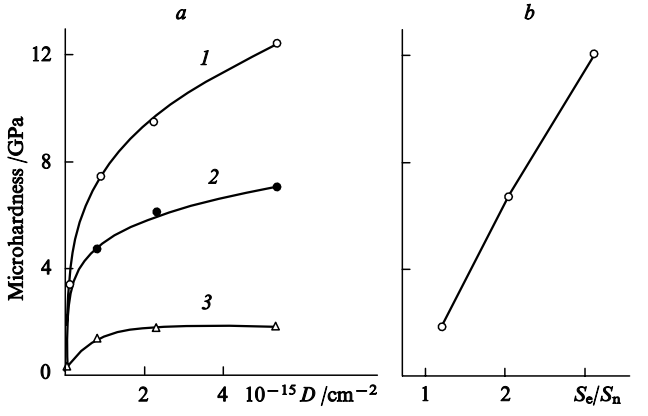


Figure 7. Microhardness of a polystyrene surface irradiated with Ar^+ ions plotted as a function of irradiation dose (*a*) and of the relative weight of energy transferred from the incident ion to polymer by electronic excitations and nuclear collisions (*b*).[122]
Ion energy /keV: 1000 (*1*), 500 (*2*) and 200 (*3*).

One of the most important consequences of ion implantation is the onset of conductivity of initially dielectric polymers. It is of great importance that the conductivity of irradiated polymers is due to the formation of carbon-containing structures in the implanted layer rather than ion doping. Therefore the conductivity, which is proportional to the optical absorption of the carbonaceous phase,[131] only indirectly depends on the nature of implanted ions, being mainly determined by the energy loss during the stopping of ions.[1, 17, 21, 129] Since the conducting phase in the ion-implanted layer is formed by discrete carbon clusters and their associates, the onset of conductivity in an irradiated polymer upon build up of implantation dose has a threshold character (see Fig. 3) and the transition from dielectric to conductor can be considered as percolation transition.[5, 17, 29, 132] The dependence of the dc conductivity, σ, on the implantation dose is given by the formula:[1, 17, 29, 132]

$$\sigma \sim (D - D_c)^t,$$

where D_c is the critical dose corresponding to the percolation threshold.

Thermoradiolysis in the implanted layer occurs under conditions of gradual coverage of the surface of polymeric target with ion tracks. Nevertheless, the formation of an infinite conducting cluster is, as a rule, observed at implantation doses corresponding to a smaller fraction of the surface covered with ion tracks compared to those predicted by the two-dimensional percolation problem. For instance, the percolation threshold for polyimide irradiated with 500 keV N^+ ions corresponds to a coverage factor of 0.3 (see Ref. 29), whereas theory predicts that percolation in an ideal two-dimensional system must occur at a critical coverage of $\sim$0.45. This suggests some ordering in the carbonaceous phase and is also supported by large values of the exponent t in the above-mentioned formula for the polymers that are prone to form carbon clusters [polyimide,[29] polyacrylonitrile,[17] poly(2,6-dimethylphenylene oxide),[17] molecular films based on perylene derivatives [18]]. In this case, the t values estimated from the slope of the linear dependence $\log\sigma \sim \log(D - D_c)$ can be as high as 4–5 if energy deposition during implantation occurs mainly by nuclear collisions and even as high as 7–8 if the electronic stopping prevails. On the other hand, for poorly carbonised polyethylene irradiated with 100 keV B^+ ions the percolation threshold corresponds to $D_c = 1.5 \times 10^{15}$ cm^{-2} (*i.e.*, in this case, $D_c > D_f$) and the exponent t in the above-mentioned formula does not exceed a value of 2.[75, 133]

As the irradiation dose increases, a system of conducting 'islands' separated by potential barriers is formed within the implanted layer.[1, 18, 134] The nanostructured carbonaceous phase formed in the immediate vicinity of the percolation threshold acquires semiconductor properties.[135] Studies of temperature dependence of the conductivity of some irradiated polymers [polyethylene, poly(ether ether ketone),[21, 136] *etc.*] showed that the formation of developed carbonaceous phase at high implantation doses causes transition from one-dimensional to three-dimensional conductivity. A similar phenomenon was observed for polyimide heavily implanted with 90 keV N^+ ions [56] and for polyamide-6 irradiated with 150 keV Sb^+ ions.[49] For polymers which are prone to undergo carbonisation during irradiation [*e.g.*, poly(*p*-phenylenebenzobisoxazole), poly(*p*-phenylenebenzobisthiazole), poly(benzimidazobenzophenanthroline)], the conductivity of the ion-implanted layer formed at high implantation dose (Kr^+, 200 keV, $D = 4 \times 10^{16}$ cm^{-2}) is close to the metal conductivity.[137, 138]

At implantation doses close to D_c, the conductivity of implanted polyethylene can be increased by 3 orders of magnitude by diffusion doping with molecular iodine.[80] However, the doping effect is unstable and ion-implanted polyethylene takes the initial value of the electrical resistance much faster than changes in the concentration of the trapped iodine diffusing out of the implanted layer occur.[139] It should be noted that it is difficult for molecular iodine vapours to penetrate the implanted layer in heavily irradiated polymers due to destruction of the system of track channels caused by the formation of the carbon nanophase.[81, 139] Doping of irradiated polyethylene with $FeCl_3$ [84] and treatment of ion-implanted polyimide with molecular chlorine lead to an increase in the conductivity by two orders of magnitude (despite the fact that addition of chlorine to some unsaturated bonds occurs simultaneously in the latter case).[140]

The conductivity of the implanted layer is strongly dependent on the peculiarities of the morphology of the carbonaceous phase (the size of carbon clusters, character of their linking in aggregates, the presence of heteroatoms). As a result, the electrical resistance of different polymers that were ion implanted under the same conditions can differ by several orders of magnitude, *e.g.*, the specific resistance of polyethylene and polyimide irradiated with 1 MeV Xe^+ ions ($D = 10^{16}$ cm^{-2}), is 6.8×10^{-3} and 30 Ω cm, respectively (see Ref. 55). The conductivity of the implanted layer

is also determined by the implantation regime and, in particular, by the energy of the implanted ions, by the presence (or absence) of forced cooling of the polymer sample (polyimide films irradiated in the absence of forced cooling have lower electrical resistance than those irradiated in the presence of forced cooling [141]), film thickness (thick films exhibit lower conductivity due to efficient cooling of the implanted layer during irradiation [25]). Nevertheless, a general trend is towards an increase in the conductivity of irradiated polymers with increasing energy of implanted ions. The highest conductivity is observed if energy deposition by incident ions occurs mostly by an 'electronic' mechanism.[21, 65, 123, 130, 142]

V. Prospects for practical applications of ion-implanted polymers

Initially, interest in studies of the effect of ion irradiation on polymers was due to fabrication of resists (both negative and positive) for lithographic processes with submicron resolution. Detailed reviews concerning the cross-linking–chain scission effects observed at very low implantation doses (10^{11}–10^{12} cm^{-2}) and responsible for changes in the solubility of irradiated polymers have been reported.[1, 143] On the other hand, the possibility of initiation of essentially different radiolytic and thermoradiolytic processes (cross-linking–fragmentation of polymer chains at low implantation doses, transformations of functional groups at implantation doses comparable with D_f and carbonisation of polymers at high implantation doses) by ion irradiation allows control of the sorption, tribological, optical and conducting properties of the polymer surface. This opens up new fields of practical applications of polymeric materials.

Implantation of PETP with heavy high-energy ions is accompanied by the formation of latent tracks in the polymer. This makes possible perforation of polymer films 10–20 μm thick by hydrolytic etching and fabrication of membranes with a controllable number of identical pores.[144–146] The pore diameter can be varied over a wide range (0.01–5 μm) by varying the duration of etching. Studies of the character of energy loss of α-particles in perforated PETP films obtained using this procedure allowed one to trace the changes in the shape of membrane channels in different stages of etching.[147] It was found that the channels have rather long cylindrical sections (up to 2/3 of the overall thickness of the polymer film) that are transformed into conical pore mouths.[147] Cylindrical channels with smooth walls can also be formed by etching ion irradiated polyimide in the presence of hydrogen peroxide [148] and hypochlorites.[149] On the other hand, typical of many polymers [*e.g.*, poly(methyl methacrylate),[148] polycarbonate,[146] *etc.*] is the formation of channels with irregular shape and broad size distribution. High uniformity of etching channels in PETP is due to some features of latent track structure.[146, 150, 151] The track core, which is at most several nanometers in radius, represents a degraded, rapidly soluble polymer containing a large number of isolated pores [152] and surrounded by a shell of radiochemically cross-linked polymer.[80, 146, 150] The shell diameter is 50 to 60 nm for implantation of xenon ions (1 MeV per nucleon) and is much larger than the penumbra diameter.[80, 150] This can be explained by the formation of cross-links due to recombination of macroradicals formed in the interaction of polymer chains with knock-on hydrogen atoms [146] (including those formed as a result of hydrodynamic shock accompanying the passage of high-energy heavy ions [153]). Probably, high spatial selectivity of etching is to some extent due to ordering of the polymer structure as a result of reorientation of the macromolecules along the ion tracks.[63] It should be noted that forced orientation of polymer molecules along the direction of ion flux can be observed not only during implantation of high-energy ions, but also in the case of ion irradiation with energies of the order of several kiloelectron-volts [154] at a fluence of $\sim 5 \times 10^{15}$ cm^{-2}.

The formation of surface pores, changes in the polar component of the surface free energy and the appearance of specific adsorption sites as a result of ion bombardment can have both positive [52, 155–162] and negative [156] effects on the efficiency of adsorption of living cells on the polymer surfaces (*e.g.*, polystyrene,[156, 158, 159] polyurethane,[160, 161] polymethylsiloxane,[52] collagen,[156, 162] *etc.*). This opens up new possibilities of control of biocompatibility of polymeric materials. As a rule, cell adsorption efficiency nonmonotonically depends on the implantation dose (*i.e.*, it is determined not only by the effects of changes in hydrophilicity) and reaches a maximum value at implantation doses that are somewhat lower than D_f.[158, 160] It was also shown that changes in the dynamics of plasma protein adsorption on the surface of silicon rubber induced by irradiation with 150 keV H_2^+, N_2^+, Na^+ and Ne^+ ions leads to nearly complete suppression of thrombogenicity.[163]

At low ion implantation doses, the refractive index, n, of a polymer increases with the polymer density. In some instances a relative increase in the refractive index can be substantial. In particular, poly(methyl methacrylate) is known to lose methoxy groups upon ion irradiation and undergo gradual transformation into an analogue of cross-linked polyethylene.[164] For this polymer, the $\Delta n/n$ ratio can be as high as 0.3 (see Refs 165 and 166) and the dependence of the refractive index on the implantation dose is nearly linear up to $D \approx 10^{15}$ cm^{-2}. At higher doses, the polymer becomes turbid due to carbonisation.[166] This allows the formation of light guides and other optical devices (couplers, interferometers) on the polymer surface.[167–169] It is of great importance that the use of high-energy ions characterised by a shift of maximum energy loss towards the track end allows fabrication of 'buried' (including crossed) light guide structures at a depth from several to several tens of micrometres under the surface of a polymer sample (depending on the energy of implanted ions).[167, 170]

Fabrication of nonlinear optical devices in the form of metal particles dispersed in a dielectric matrix [171] by implantation of polymer with corresponding metal ions is a difficult task since the optical density of the polymeric host increases with the implantation dose. On the other hand, one can expect that the formation of a metal nanophase during ion irradiation of the polymers containing chemically bound metal ions will occur at low implantation doses.

As mentioned above, carbonisation of polymers at high implantation doses leads to a substantial increase in their microhardness,[28] which can be as high as 22 GPa [123] (*cf.* a value of less than 12 GPa for martensite steel) and is comparable with the hardness of diamond-like carbon films. The best results were obtained in the case of simultaneous implantation of ions with different mass and energy, *i.e.*, characterised by different penetration depth and responsible for different degrees of carbonisation of polymers.[28] An increase in hardness of the surface of implanted polymers [polyimide,[123, 126, 172] polystyrene,[122, 123] polycarbonate,[128, 173] pristine [92, 127] and partially fluorinated polyethylene,[23] poly(2,6-dimethylphenylene oxide),[174] *etc.*] is accompanied by reduction of their electrical resistance [122] and causes substantial improvement of wear resistance.[122, 124] The latter parameter nonmonotonically depends on implantation dose since an increase in hardness of the implanted layer makes it more brittle and causes a gradual decrease in its adhesion to the polymeric support. The dramatic decrease in the friction coefficient upon ion irradiation observed for polycarbonate [173, 175] and poly(2,6-dimethylphenylene oxide) [174] seems to be to a great extent due to an increase in hydrophilicity of the polymer surface, which favours the formation of a surface layer of chemisorbed water with good antifrictional properties.

The carbonised surface layer substantially improves the chemical stability of irradiated polymers towards organic solvents; however, this layer is porous and therefore provides no perfect protection of the polymeric support.[176] High-dose implantation of low-energy (25–40 keV) Si^+, Al^+, Y^+, Y^{2+} and Y^{3+} ions leads to suppression of erosion of the surface of polyimide, PETP and some other polymers exposed to a flux of oxygen atoms (under conditions corresponding to Earth orbit space environment) due to the formation of a composite oxide-carbon coating.[177]

Polymers irradiated to high doses represent an unusual electrode material, the surface properties of which can vary depending on the ratio of the concentrations of sp^2- and sp^3-hybridised carbon atoms in the implanted layer. Since the carbon clusters responsible for conductivity of the implanted layer are small, their oxidation under anodic polarisation observed in the absence of depolarisers is accompanied by irreversible loss of the electrochemical activity of irradiated polymers.[75] On the other hand, for initially conducting polymers (polyaniline,[178] polypyrrole,[179] polythiophene,[180] polybithiophene,[181] polyethoxythiophene,[182] polyethylenedioxythiophene[182]) that lose their electrochemical activity as a result of degradation of the π-electron system at low implantation doses ($D < 10^{15}$ cm^{-2})[180] the surface of the polymeric electrode exhibits recovery under anodic polarisation due to electrochemical oxidation of the carbonaceous phase.[179, 181, 183] The possibility of ion-induced passivation of conducting polymers towards the processes of electrochemical polymerisation[181, 183] and electrochemical deposition of metals[179, 180, 182] allows one to change the surface profile of polymeric electrodes[181] and to form metal patterns with micrometre resolution.[179, 180, 182]

The possibility of varying the conducting properties of implanted polymers opens up new prospects for fabrication of microelectronic systems including the formation of conducting strips on the surface of polymeric materials,[184] fabrication of planar resistors with variable electrical resistance which can be varied over a wide range,[2] thermistors and bolometers.[2] Ion implantation can be used for development of more complex polymer-based electronic devices, namely, diodes and transistors. It is of great importance for fabrication of polymeric electronic devices (in particular, $p-n$-junctions[185, 186] and conducting channels of field-effect transistors[187]) that many of the initially conducting polymers with well-developed π-electron conjugation systems [*e.g.*, poly(*p*-phenylenevinylene), polyacetylene][186, 187] exhibit resistance towards ion-induced dehydrogenation. Therefore, they can be doped by implantation of ions with medium-range energies ($\sim$30 keV). Under these conditions, purely chemical doping of *p*-type for implantation of iodine ions and of *n*-type for implantation of alkali metal ions can be accompanied by the effects associated with the formation of structural defects in the polymer matrix (*e.g.*, as a result of electron capture from the π valence band of polyparaphenylene by the lower-lying sp^2-electron energy levels corresponding to dangling bonds of carbon atoms[188]). The possibility of fabrication of unusual electronic switching devices (analogues of field-effect transistors[3, 75, 94, 96]) based on implanted, initially dielectric polymers (polyethylene, polyamide-6) with a 'buried' carbonaceous phase separated from the surface by a dielectric layer $\sim$10 nm thick was also demonstrated. This layer can be made more uniform by electrochemical polymerisation of dielectric poly(*o*-phenylenediamine) in the pores of the implanted layer.[75] The spatial characteristics of this structure allow the 'buried' layer to act as a conducting channel of the field-effect transistor. The ac resistance of such a channel changed by more than four orders of magnitude upon applying an external electric field.[3, 75, 94]

VI. Conclusion

The above-mentioned experimental results indicate that ion irradiation of polymers causes some specific phenomena that currently should be considered within the framework of a special division of high-energy chemistry. Ion-induced processes in polymeric targets represent a kind of pulse thermoradiolysis which occurs in the subnanosecond time scale and sometimes under conditions of massive ('non-thermodynamic') breakage of chemical bonds by nuclear collisions. The energy deposited by the incident ions in the polymer matrix is rather high; however, carbonisation of the polymer surface observed in this case cannot be reduced to simple 'graphitisation' of the polymer within the track of the stopping ion.

The formation of the carbonaceous phase on the polymer surface with an increase in the implantation dose involves some consecutive stages essentially differing in character of the corresponding ion-induced reactions. These stages include (1) dehydrogenation of a polymer (this occurs, as a rule, simultaneously with the radiation-induced cross-linking of the polymer) and transformation of functional groups, which results in the formation of 'pre-carbon' structures; (2) growth of carbon clusters, the limiting size of which is determined by the energy of implanted ions; (3) aggregation of carbon clusters and the formation of conjugated and non-conjugated bonds. The energy loss of high-energy ions affects the composition of the newly formed nanostructured carbonaceous phase more than the nature of the irradiated polymer. On the other hand, subtle variations of the short- and medium-range order of the carbonaceous nanophase, which determine such fundamental properties as conductivity and microhardness, depend on the mechanism of ion-induced thermoradiolysis and are very sensitive to the composition of the irradiated polymeric target. By and large, this type of influence of the polymer nature on the properties of ion implantation products can be considered as specific memory effect.

Figure 8 presents a diagram which qualitatively outlines main consequences of ion irradiation of polymers. By varying the irradiation dose one can control the rheologocal, sorption, conducting, electrochemical and optical properties of polymers and their microhardness, wear resistance and biocompatibility.

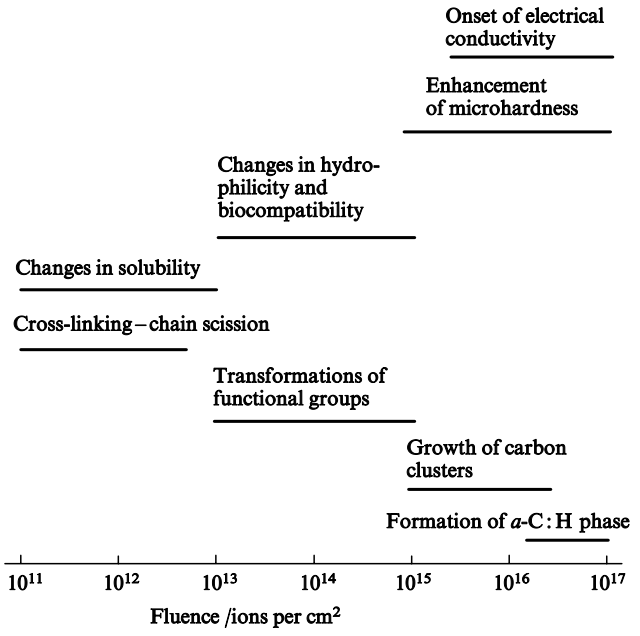


Figure 8. Principal transformations in the implanted layer and related changes in the physical and chemical properties of the polymer surface irradiated with different ion doses at energies between 0.1 and 1 MeV.

Thus, ion irradiation is a promising method of targeted modification of polymer surfaces. Build up of implantation doses causes processes of fundamentally different nature which can be controlled by varying the energy and masses of the implanted ions. All potentialities of this experimental technique and detailed mechanisms of physicochemical processes accompanying ion implantation of polymeric materials require further study.

The author expresses his gratitude to the Basic Research Foundation of Belarus for financial support of the experiments on the synthesis of nanostructured carbon materials by ion implantation techniques.

References

1. T Venkatesan, L Calcagno, B S Elman, G Foti, in *Ion Beam Modification of Insulators* (Eds P Mazzoldi, G W Arnold) (Amsterdam: Elsevier, 1987) p. 301
2. R E Giedd, M G Moss, J Kaufmann, Y Q Wang, in *Electrical and Optical Polymer Systems* (Eds D L Wise, G E Wnek, D J Trantolo, T M Cooper, J G Gresser) (New York: Marcel Dekker, 1998) p. 1011
3. D V Sviridov, I P Kozlov, V B Odzhaev, in *Electrical and Optical Polymer Systems* (Eds D L Wise, G E Wnek, D J Trantolo, T M Cooper, J G Gresser) (New York: Marcel Dekker, 1998) p. 387
4. V B Odzhaev, I P Kozlov, V N Popok, D V Sviridov *Ionnaya Implantatsiya v Polimery* (Ion Implantation in Polymers) (Minsk: Belarusian State University, 1998)
5. J Davenas, P Thevenard *Nucl. Instrum. Methods Phys. Res. B* **80**/**81** 1021 (1993)
6. G Marletta, F Iacona, in *Materials and Processes for Surface and Interface Engineering (NATO ASI Series, Series E: Appl. Sci.)* (Ed. Y Pauleau) (Dordrecht: Kluwer Academic, 1995) Vol. 290, p. 597
7. E H Lee *Nucl. Instrum. Methods Phys. Res. B* **151** 29 (1999)
8. J P Biersack In *Materials and Processes for Surface and Interface Engineering (NATO ASI Series, Series E: Appl. Sci.)* (Ed. Y Pauleau) (Dordrecht: Kluwer Academic, 1995) Vol. 290, p. 39
9. E J Kobetich, R Katz *Phys. Rev.* **170** 391 (1968)
10. J L Magee, A Chatterjee *J. Phys. Chem.* **84** 3529 (1980)
11. A Mozumder *J. Chem. Phys.* **60** 1145 (1974)
12. V V Katin, Yu V Martynenko, Yu N Yavlinskii *Zh. Tekhn. Fiz.* **59** (12) 88 (1989) [a]
13. G J Dienes, G H Vineyard *Radiation Effects in Solids* (New York: Interscience, 1957)
14. A Mozumder *Adv. Radiat. Chem.* **1** 1 (1969)
15. R R Lucchese *J. Chem. Phys.* **86** 443 (1987)
16. I S Bitensky, P Demirev, B U R Sundquist *Nucl. Instrum. Methods Phys. Res. B* **82** 356 (1993)
17. B Wasserman *Phys. Rev. B* **34** 1926 (1986)
18. M L Kaplan, S R Forrest, P H Schmidt, T Venkatesan *J. Appl. Phys.* **55** 732 (1984)
19. G Schiwietz, G Xiao, P L Grande, E Luderer, R Pazirandeh, U Stettner *Nucl. Instrum. Methods Phys. Res. B* **146** 131 (1998)
20. E H Lee, D M Hembree Jr, G R Rao, L K Mansur *Phys. Rev. B* **48** 15540 (1993)
21. C J Sofield, S Sugden, J Ing, L B Bridwell, Y Q Wang *Vacuum* **44** 285 (1993)
22. G Foti, R Reitano *Nucl. Instrum. Methods Phys. Res. B* **46** 306 (1990)
23. G R Rao, Z L Wang, E H Lee *J. Mater. Res.* **8** 927 (1993)
24. M B Lewis, E H Lee *Nucl. Instrum. Methods Phys. Res. B* **61** 457 (1991)
25. I H Loh, W R Oliver, P Sioshansi *Nucl. Instrum. Methods Phys. Res. B* **34** 337 (1988)
26. L Calcagno, G Foti *Appl. Phys. Lett.* **47** 383 (1985)
27. T Venkatesan, S R Forrest, M L Kaplan, C A Murray, P H Schmidt, B J Wilkens *J. Appl. Phys.* **54** 3150 (1983)
28. E H Lee, M B Lewis, P J Blau, L K Mansur *J. Mater. Res.* **6** 610 (1991)
29. J Davenas *Mol. Cryst. Liq. Cryst.* **186** 231 (1990)
30. D K Avasthi, J P Sing, A Biswas, S K Bose *Nucl. Instrum. Methods Phys. Res. B* **146** 504 (1998)
31. T Seguchi, N Hayakawa, K Yoshida, N Tamura *Radiat. Phys. Chem.* **26** 221 (1985)
32. A Licciardello, M E Fragala, G Compagnini, O Puglisi *Nucl. Instrum. Methods Phys. Res. B* **122** 589 (1997)
33. N A Bakh, A V Vannikov, A D Grishina, Z A Markova, S V Nizhnii, in *Radiatsionnaya Khimiya Polimerov* (Radiation Chemistry of Polymers) (Moscow: Nauka, 1966) p. 263
34. V Picq, E Balanzat *Nucl. Instrum. Methods Phys. Res. B* **151** 76 (1999)
35. V Hnatowicz, J Kvítek, V Švorčík, V Rybka *Appl. Phys. A* **58** 349 (1994)
36. V Hnatowicz, V Peřina, V Havránek, V Voseček, J Novotný, J Vacík, V Švorčík, V Rybka, A Kluge *Nucl. Instrum. Methods Phys. Res. B* **161**–**163** 1099 (2000)
37. G Brinkmalm, P Demirev, D Fengoe *Phys. Rev. B* **47** 7560 (1993)
38. L T Chadderton, D Fink, H J Möckel, K K Dwivedi, A Hammoudi *Radiat. Eff. Defects Solids* **127** 163 (1993)
39. L T Chadderton, D Fink, Y Gramaly, H J Möckel, L Wang, H Omichi, F Hosoi *Nucl. Instrum. Methods Phys. Res. B* **91** 71 (1994)
40. K-H Homann *Angew. Chem., Int. Ed.* **37** 2434 (1998)
41. Yu E Lozovik, A M Popov *Usp. Fiz. Nauk* **167** 751 (1997) [b]
42. C J Pope, J A Marr, J B Howard *J. Phys. Chem.* **97** 11001 (1993)
43. N S Goroff *Acc. Chem. Res.* **29** 77 (1996)
44. C Z Wang, C H Xu, C T Chan, K M Ho *J. Phys. Chem.* **96** 3563 (1992)
45. B M Bulychev, I A Udod *Ross. Khim. Zh.* **39** 9 (1995) [c]
46. S E Stein, A Fahr *J. Phys. Chem.* **89** 3714 (1985)
47. H D Beckhaus, C Ruchardt, M Kao, H F Diederic, C S Foote *Angew. Chem.* **104** 69 (1992)
48. T Steckenreiter, E Balanzant, H Fuess, C Trautmann *Nucl. Instrum. Methods Phys. Res. B* **151** 161 (1999)
49. V Švorčík, V Rybka, I Míéek, V Popok, O Jankovskij, V Hnatowicz, J Kvítek *Eur. Polym. J.* **30** 1411 (1994)
50. Jizhong Zhang, Xiaoyan Ye, Xiaojun Yu, Hengde Li *Mater. Sci. Eng. B* **84** 200 (2001)
51. E Fitzer, K Mueller, W Schaefer, in *Chemistry and Physics of Carbon. A Series of Advances* Vol. 7 (New York: Marcel Dekker, 1971) p. 237
52. C Satriano, E Conte, G Marletta *Langmuir* **17** 2243 (2001)
53. S S Eskildsen, G Sshrensen *Nucl. Instrum. Methods Phys. Res. B* **7**/**8** 481 (1985)
54. I G Kaplan, V G Plotnikov *Khim. Vys. Energ.* **1** 507 (1967) [d]
55. J Davenas, X L Xu, G Boiteux, D Sage *Nucl. Instrum. Methods Phys. Res. B* **39** 754 (1989)
56. V Švorčík, R Endršt, V Rybka, E Arenholz, V Hnatowicz, F Černý *Eur. Polym. J.* **31** 189 (1995)
57. V Švorčík, K Prošková, V Hnatowicz, E Arenholz, A Kluge *Polym. Degrad. Stab.* **65** 131 (1999)
58. K Sahre, K-J Eichhorn, F Simon, D Pleul, A Janke, G Gerlach *Surf. Coat. Technol.* **139** 257 (2001)
59. G Marletta, S Pignataro, A Tóth, I Bertéti, T Székely, B Keszler *Macromolecules* **24** 99 (1991)
60. F Iacona, G Marletta *Nucl. Instrum. Methods Phys. Res. B* **166**–**167** 676 (2000)
61. V Švorčík, R Endršt, V Rybka, V Hnatowicz, F Černý *J. Electrochem. Soc.* **141** 582 (1994)
62. V Švorčík, V Rybka, V Hnatowicz, J Kvítek *Mater. Lett.* **19** 329 (1994.)
63. M Eßer, J Fuhrmann *Nucl. Instrum. Methods Phys. Res. B* **151** 118 (1999)
64. G Marletta *Nucl. Instrum. Methods Phys. Res. B* **46** 295 (1990)
65. L B Bridwell, R E Giedd, W Yongqiang, S S Mohite, T Jahnke, I M Brown *Nucl. Instrum. Methods Phys. Res. B* **59**/**60** 1240 (1991)
66. G Marletta, F Iacona *Nucl. Instrum. Methods Phys. Res. B* **80**/**81** 1405 (1993)
67. G Marletta, F Iacona, A Toth *Macromolecules* **25** 3190 (1992)
68. A M Ektessabi, S Hakamata *Thin Solid Films* **377**–**378** 621 (2000)
69. D Fink, K Ibel, P Goppelt, V Biersack, L Wang, M Behar *Nucl. Instrum. Methods Phys. Res. B* **46** 342 (1990)
70. O Yu Posudievskii, I G Myasnikova, A A Chuiko *Dokl. Akad. Nauk SSSR* **319** 196 (1991) [e]
71. L Calcagno, G Foti *Nucl. Instrum. Methods Phys. Res. B* **59**/**60** 1153 (1991)
72. I P Kozlov, V B Odzhaev, I A Karpovich, V N Popok, D V Sviridov *Zh. Prikl. Spektrosk.* **65** 377 (1998)
73. J Robertson *Adv. Phys.* **35** 317 (1986)
74. B Wasserman, M S Dresselhaus, G Braunstein, G E Wnek, G Roth *J. Electron. Mater.* **14** 157 (1985)
75. I I Azarko, I A Karpovich, I P Kozlov, V B Odzhaev, D V Sviridov *Poverkhnost* 80 (1999)
76. O Yu Posudievskii, I G Myasnikova, A A Chuiko *Dokl. Akad. Nauk SSSR* **321** 146 (1991) e
77. F F Komarov, A V Leontyev, V V Grigorev *Nucl. Instrum. Methods Phys. Res. B* **166**–**167** 650 (2000)
78. I I Azarko, V Hnatowicz, I P Kozlov, E I Kozlova, V B Odzhaev, V N Popok *Phys. Status Solidi* **146** K23 (1994)
79. I I Azarko, I A Karpovich, I P Kozlov, V B Odzhaev, V N Popok, D V Sviridov, in *Proceedings of the 209th ACS National Meeting, Anaheim, USA, 1995* p. 337

80. A I Vilensky, O G Larionov, R V Gainutdinov, A L Tolstikhina, V Ya Kabanov, D L Zagorski, E V Khataibe, A N Netchaev, B V Mchedlishvili *Radiat. Measurements* **34** 75 (2001)
81. J Davenas, X L Xu *Nucl. Instrum. Methods Phys. Res. B* **71** 31 (1992)
82. V Hnatowicz, J Vacík, V Peřina, V Švorčík, V Rybka, V Popok, O Jankovskij, D Fink, R Klett *Radiat. Measuriments* **25** 71 (1995)
83. V Hnatowicz, J Kvìtek, V Peřina, V Švorčík, V Rybka, V Popok *Nucl. Instrum. Methods B* **93** 282 (1994)
84. V Švorčík, E I Kozlova, V Rybka, V Hnatowicz *Mater. Lett.* **23** 321 (1995)
85. V Hnatowicz, J Kvìtek, V Švorčík, V Rybka, V Popok *J. Appl. Polym. Sci.* **55** 451 (1995)
86. V Hnatowicz, J Vacík, V Rybka, V Popok, V Švorčík, D Fink, D Klett, in *Proceedings of the International Symposium 'Ionizing Radiation and Polymers', Guadeloupe, France, 1994* p. 96
87. V Švorčík, V Hnatowicz, P Stopka, L Bačková, J Heitz, R Öchsner, H Ryssel *Radiat. Phys. Chem.* **60** 89 (2001)
88. V Švorčík, V Rybka, R Endršt, V Hnatowicz, J Kvìtek *J. Electrochem. Soc.* **140** 542 (1993)
89. V Hnatowicz, J Kvìtek, V Švorčík, V Rybka *Eur. Polym. J.* **29** 1255 (1993)
90. V Hnatowicz, J Kvìtek, V Švorčík, V Rybka, V Popok *Czech. J. Phys.* **44** 621 (1994)
91. G-H Wang, G-Q Pan, L Dou, R-X Yu, T Zhang, S-G Jiang, Q-L Dai *Nucl. Instrum. Methods Phys. Res. B* **27** 410 (1987)
92. O N Tretinnikov, Y Ikada *J. Polymer Sci.* **36** 715 (1998)
93. V N Popok, V B Odzhaev, I P Kozlov, I I Azarko, I A Karpovich, D V Sviridov *Nucl. Instrum. Methods Phys. Res. B* **129** 60 (1997)
94. V N Popok, I A Karpovich, V B Odzhaev, D V Sviridov *Nucl. Instrum. Methods Phys. Res. B* **148** 1106 (1999)
95. V B Odzhaev, I I Azarko, I A Karpovich, I P Kozlov, V N Popok, D V Sviridov, V Hnatowicz, O Jankovskij, V Rybka, V Švorčík *Mater. Lett* **23** 163 (1995)
96. V N Popok, V B Odzhaev, I I Azarko, I P Kozlov, D V Sviridov *Nucl. Instrum. Methods Phys. Res. B* **166–167** 660 (2000)
97. D Fink, M Müller, U Stettner, M Behar, P F P Fichtner, F C Zawislak *Nucl. Instrum. Methods Phys. Res. B* **32** 1 50 (1988)
98. R B Guimaraes, L Amaral, M Behar, F C Zawislak, D Fink *Nucl. Instrum. Methods Phys. Res. B* **39** 800 (1989)
99. J Vacík, V Hnatowicz, J Červená, V Peřina, V Popok, V Odzhaev, D Fink *Nucl. Instrum. Methods Phys. Res. B* **148** 1126 (1999)
100. V Hnatowicz, J Vacík, J Červená, V Peřina, V Švorčík,V Rybka *Nucl. Instrum. Methods Phys. Res. B* **136–138** 568 (1998)
101. T Hioki, S Noda, M Sugiura, M Kakeno, K Yamada, J Kawamoto *Appl. Phys. Lett.* **43** 30 (1983)
102. J R Kaschny, L Amaral, D Fink, M Behar *Radiat. Eff. Defects Solids* **125** 289 (1993)
103. M Behar, L Amaral, J R Kaschny, F C Zawislak *Phys. Lett. A* **148** 104 (1990)
104. Yu I Gudimenko, E V Kotov, V E Agabekov, E V Boiko *Poverkhnost* 119 (1994)
105. M Behar, P F P Fichtner, P L Grande, F C Zawislak *Mater. Sci. Eng. R Rep.* **15** 1 (1995)
106. D Fink, M Müller, S Ghosh, V Hnatowicz, J Vacík *Appl. Phys. A* **68** 429 (1999)
107. J P Biersack, L G Haggmark *Nucl. Instrum. Methods Phys. Res. B* **174** 257 (1980)
108. V N Popok, I I Azarko, V B Odzhaev, A Tóth, R I Khaibullin *Nucl. Instrum. Methods Phys. Res. B* **178** 305 (2001)
109. P L Timms *Adv. Inorg. Chem. Radiochem.* **14** 121 (1972)
110. J Vacík, V Hnatowicz, J Červená, V Peřina, V Popok, V Odzhzaev, V Švorčík, V Rybka, E Arenholz, D Fink *Nucl. Instrum. Methods Phys. Res. B* **166–167** 637 (2000)
111. D Fink, M Müller, A Schmoldt, J K Zhou, L T Chadderton, X L Xu *Nucl. Instrum. Methods Phys. Res. B* **65** 432 (1992)
112. V Petkunov, V Zhikharev, M Ibragimova, E Zheglov, V Bazarov, I Khaibullin *Solid State Commun.* **97** 361 (1996)
113. A L Stepanov, S N Abdullin, V Yu Petkunov, Yu N Osin, R I Khaibullin, I B Khaibullin *Philos. Mag. B* **80** 23 (2000)
114. S N Abdullin, A L Stepanov, Yu N Osin, R I Khaibullin, I B Khaibullin *Surf. Coat. Technol.* **106** 214 (1998)
115. R I Khaibullin, Yu N Osin, A L Stepanov, I B Khaibullin *Nucl. Instrum. Methods Phys. Res. B* **148** 1023 (1999)
116. R I Khaibullin, Yu N Osin, A L Stepanov, I B Khaibullin *Vacuum* **51** 289 (1998)
117. I B Khaibullin, R I Khaibullin, S N Abdullin, A L Stepanov, Yu N Osin, V V Bazarov, S P Kuzin *Nucl. Instrum. Methods Phys. Res. B* **127/128** 685 (1997)
118. B Z Rameev, B Aktas, R I Khaibullin, V A Zhikarev, Yu N Osin, I B Khaibullin *Vacuum* **58** 551 (2000)
119. K Yoshida, M Iwaki *Nucl. Instrum. Methods Phys. Res. B* **19–20** 878 (1987)
120. T Kobayashi, T Iwata, Y Doi, M Iwaki *Nucl. Instrum. Methods Phys. Res. B* **175–177** 548 (2001)
121. M Iwaki *Nucl. Instrum. Methods Phys. Res. B* **175–177** 368 (2001)
122. E H Lee, G R Rao, M B Lewis, L K Mansur *Nucl. Instrum. Methods Phys. Res. B* **74** 326 (1993)
123. G R Rao, E H Lee *J. Mater. Res.* **11** 2661 (1996)
124. H Dong, T Bell *Surf. Coat. Technol.* **111** 29 (1999)
125. J C Pivin *Nucl. Instrum. Methods Phys. Res. B* **127** 685 (1997)
126. J S Chen, S P Lau, Z Sun, B K Tay, G Q Yu, F Y Zhu, D Z Zhu, H J Xu *Surf. Coat. Technol.* **138** 33 (2001)
127. G R Rao, K Monar, E H Lee, J R Treglio *Surf. Coat. Technol.* **64** 69 (1994)
128. E Yap, D G McCulloch, D R McKenzie, M V Swain, L S Wielunski, R A Clissold *J. Appl. Phys.* **83** 3404 (1998)
129. C J Bedell, C J Sofield, L B Bridwell, I M Brown *J. Appl. Phys.* **67** 1736 (1990)
130. R Öchsner, A Kluge, S Zechel-Malonn, L Gong, H Ryssel *Nucl. Instrum. Methods Phys. Res. B* **80/81** 1050 (1993)
131. K Sakamoto, M Iwaki, K Takahashi *J. Mater. Res.* **11** 2656 (1996)
132. F H Ruddy, J Bartko, K F Schoch Jr *J. Mater. Res.* **3** 1253 (1988)
133. D V Sviridov, Doctoral Thesis in Chemical Sciences, Belarusian State University, Minsk, 1999
134. P Sheng, E K Sichel, J I Gittleman *Phys. Rev. Lett.* **40** 1197 (1978)
135. A De Bonis, A Bearzotti, G Marletta *Nucl. Instrum. Methods Phys. Res. B* **151** 101 (1999)
136. Y Q Wang, S S Mohite, L B Bridwell, R E Giedd, C J Sofield *J. Mater. Res.* **8** 388 (1993)
137. G Du, V N Prigodin, A Burns, J Joo, C S Wang, A J Epstein *Phys. Rev. B* **58** 4485 (1998)
138. G Du, A Burns, V N Prigodin, C S Wang, J Joo, A J Epstein *Phys. Rev. B* **61** 10142 (2000)
139. O Jankovskij, V Švorčík, V Rybka, V Hnatowicz, V Popok *Nucl. Instrum. Methods Phys. Res. B* **95** 192 (1995)
140. V Švorčík, V Rybka, I Stibor, V Hnatowicz *J. Electrochem. Soc.* **142** 590 (1995)
141. A N Aleshin, A V Gribanov, A V Dobrodumov, A V Suvorov, I S Shlimak *Fiz. Tverd. Tela* **31** 12 (1989) [f]
142. K-H Bäther, U Herrmann *Surf. Coat. Technol.* **74–75** 670 (1995)
143. E Reichmanis, L F Thompson *Chem. Rev.* **89** 1273 (1989)
144. G N Flerov *Vestn. Akad. Nauk SSSR* 35 (1984) [g]
145. R Spohr *Ion Tracks and Microtechnology* (Braunschweig: Vieweg, 1990)
146. P Yu Apel' *Khim. Vys. Energ.* **25** 132 (1991) [d]
147. J Vacík, J Červená, V Hnatowicz, S Posta, D Fink, H Naramoto, Y Kobayashi, K Hirata, P Strauss *Radiat. Eff. Defects Solids* **147** 177 (1999)
148. D L Zagorskii, V V Berezkin, A I Vilenskii, T V Tsyganova, B V Mchedlishvili *Poverkhnost* 41 (2000)
149. R Sudowe, P Vater, R Brandt, J Vetter, W Ensinger *Nucl. Instrum. Methods Phys. Res. B* **175–177** 564 (2001)
150. A I Vilenskii, V A Oleinikov, B V Mchedlishvili *Khim. Vys. Energ.* **26** 300 (1992) [d]
151. P Apel, A Schulz, R Spohr, C Trautmann, V Vutsadakis *Nucl. Instrum. Methods Phys. Res. B* **146** 468 (1998)
152. Yu D Sokolova, A A Machula, V K Milinchuk, G S Zhdanov *Kolloid. Zh.* **59** 395 (1997) [h]
153. V I Gol'danskii, E Ya Lantsburg, N A Yampol'skii *Pis'ma Zh. Eksp. Teor. Fiz.* **21** 365 (1975) [i]
154. J Stöhr, M G Samant, J Lüning, A C Callegari, P Chaudhari, J P Doyle, J A Lacey, S A Lien, S Purushothaman, J L Speidell *Science* **292** 2299 (2001)
155. J D Carlson, J E Bares, A M Guzman, P P Pronko *Nucl. Instrum. Methods Phys. Res. B* **7/8** 507 (1985)

156. Y Suzuki, M Kusakabe, M Kaibara, M Iwaki, H Sasabe, T Nishisaka *Nucl. Instrum. Methods Phys. Res. B* **91** 588 (1994)
157. H Tsuji, H Satoh, S Ikeda, N Ikemoto, Y Gotoh, J Ishikawa *Surf. Coat. Technol.* **103**–**104** 124 (1998)
158. L Bačáková, V Švorčík, V Rybka, I Miėek, V Hnatowicz, V Lisá, F Kocourek *Biomaterials* **17** 1121 (1996)
159. L Bačáková, V Mares, M G Bottone, M G Pellicciari, V Lisá, V Švorčík *J. Biomed. Mater.* **49** 369 (2000)
160. L Dejuu, Z Jie, G Hanging, L Mozhu, D Fuging, Z Quing *Nucl. Instrum. Methods Phys. Res. B* **82** 57 (1993)
161. F Z Cui, Z S Luo *Surf. Coatings Technol.* **112** 278 (1999)
162. K Kurotobi, M Kaibara, Y Suzuki, M Iwaki, H Nakajima *Nucl. Instrum. Methods Phys. Res. B* **175**–**177** 791 (2001)
163. Y Suzuki, M Kusakabe, H Akiba, K Kusakabe, M Iwaki *Nucl. Instrum. Methods Phys. Res. B* **59** 698 (1991)
164. B Pignataro, M E Fragala, O Puglisi *Nucl. Instrum. Methods Phys. Res. B* **131** 141 (1997)
165. L Zhang, P D Townsend, P J Chandler, J R Kulisch *J. Appl. Phys.* **66** 4547 (1989)
166. J P Biersack, R Kallweit *Nucl. Instrum. Methods Phys. Res. B* **46** 309 (1990)
167. S Brunner, D M Rück, W F X Frank, F Linke, A Schösser, U Behringer *Nucl. Instrum. Methods Phys. Res. B* **89** 373 (1994)
168. W F X Frank, A Schoesser, S Brunner, F Linke, T K Strempel, M Eich *Proc. SPIE* **1774** 268 (1993)
169. P Cottin, R A Lessard, É J Knystautas, S Roorda *Nucl. Instrum. Methods Phys. Res. B* **151** 97 (1999)
170. D M Rück *Nucl. Instrum. Methods Phys. Res. B* **166-167** 602 (2000)
171. R F Haglund, Li Yang, R H Magruder, C W White, R A Zuhr, L Yang, R Dorsinville, R R Alfano *Nucl. Instrum. Methods Phys. Res. B* **91** 493 (1991)
172. E H Lee, G R Rao, M B Lewis, L K Mansur *J. Mater. Res.* **9** 1043 (1994)
173. J San, B Zhu, J Liu, Zh Liu, Ch Dong, Q Zhang *Surf. Coat. Technol.* **138** 242 (2001)
174. J San, J Liu, B Zhu, Zh Liu, Ch Dong, Q Zhang *Wear* **251** 1504 (2001)
175. G R Rao, P J Blau, E H Lee *Wear* **184** 213 (1995)
176. L Guzman, R Celva, A Miotello, E Voltolini, F Ferrari, M Adami *Surf. Coat. Technol.* **103**–**104** 375 (1998)
177. Z A Iskanderova, J Kleiman, W D Morison, R C Tennyson *Mater. Chem. Phys.* **54** 91 (1998)
178. Zh-M Liu, J-L Zhu, Y-P Guo, Zh-W Yu, P-P Qian, Z-T Ma *Nucl. Instrum. Methods Phys. Res. B* **91** 465 (1994)
179. S Schiestel, G K Wolf *Synth. Met.* **67** 273 (1994)
180. S Schiestel, W Ensinger, G K Wolf *Nucl. Instrum. Methods Phys. Res. B* **91** 473 (1994)
181. K G Jung, J W Schultze, K S Robinson, H Schmiedel *Fresenius J. Anal. Chem.* **353** 282 (1995)
182. T Asmus, G K Wolf *Nucl. Instrum. Methods Phys. Res. B* **166**–**167** 732 (2000)
183. K G Jung, J W Schultze, Ch Buchal *Nucl. Instrum. Methods Phys. Res. B* **80**/**81** 1076 (1993)
184. T A Tombrello *Nucl. Instrum. Methods Phys. Res. B* **94** 424 (1994)
185. T Wada, A Takeno, M Iwaki, H Sasabe, Y Kobayashi *J. Chem. Soc., Chem. Commun.* 1194 (1985)
186. S H Lin, K I Sheng, T W Rong, J R Bao, W M Wang, H H Wan, Z Y Zhou, X F Zhu, F J Yang *Nucl. Instrum. Methods Phys. Res. B* **59**/**60** 1257 (1991)
187. K Pichler, C P Jarrett, R H Friend, B Ratier, A Moliton *J. Appl. Phys.* **77** 3523 (1995)
188. A Moliton, B Lucas, C Moreau, R H Friend, B Francois *Philos. Mag. B* **69** 1155 (1994)

[a] — *Tech. Phys. (Engl. Transl.)*
[b] — *Physics-Uspekhi (Engl. Transl.)*
[c] — *Mendeleev Chem. J. (Engl. Transl.)*
[d] — *High Energy Chem. (Engl. Transl.)*
[e] — *Dokl. Chem. (Engl. Transl.)*
[f] — *Phys. Solid State (Engl. Transl.)*
[g] — *Herald Russ. Acad. Sci. (Engl. Transl.)*
[h] — *Colloid J. (Engl. Transl.)*
[i] — *J. Exp. Theor. Phys. Lett. (Engl. Transl.)*